LINEAR AND NON-LINEAR FINITE ELEMENT ERROR ESTIMATION BASED ON ASSUMED STRAIN FIELDS

F. Gabaldón[1,*] and J.M. Goicolea[1]

[1] *E.T.S. Ingenieros de Caminos, Canales y Puertos, Universidad Politécnica de Madrid, 28040 Madrid, Spain*

SUMMARY

In this work we analyse the use of enhanced strain fields for the purpose of error estimation in finite element solid mechanics applications. The proposed approach evaluates the quality of the solution for standard Galerkin displacement elements, taking into account the enrichment of the solution with enhanced assumed strain (EAS) mixed elements. The contribution of the enhanced strain modes is measured with an energy norm.

The method proposed has two interesting advantages. Firstly, it results in a local formulation which is evaluated element by element. Secondly, it is easily extended to nonlinear problems. In this work, the formulation is developed for linear elasticity, for finite strain elasticity, and von Mises small strain plasticity.

Finally, some representative numerical simulations are presented which show in practice the performance of the method.

KEY WORDS: Mixed Elements, Error Estimation, Hiperelasticity, Plasticity, Assumed Strain

1. INTRODUCTION

Finite element methods have become one of the main computational tools for applied mechanics and structural engineering. Many successful applications exist nowadays for both linear and nonlinear problems. This expansion in the field of applications must be accompanied with parallel efforts to assess the quality of the computed results.

The interest of "a posteriori" error estimators lies in their direct applicability to adaptive refinement techniques. The development of these estimators may be traced back to the works of Babuška[3] and Zienkiewicz–Zhu [19]. Since then, several error estimators have been proposed for linear analyses, whose efficiency has been proved for a wide variety of problems.

The development of nonlinear finite element methods is more recent, and a number of research lines remain open. Error estimation applied to this kind of problems has some inherent

*Correspondence to: F. Gabaldón. Departamento de Mecánica de Medios Continuos y Teoría de Estructuras. E.T.S. Ingenieros de Caminos, Canales y Puertos. C/ Profesor Aranguren s/n, Ciudad Universitaria, 28040 Madrid, Spain. e-mail: felipe@mecanica.upm.es

limitations due to the nature of nonlinear behaviour. As examples, one might cite non-unique solutions associated with load path dependency, or bifurcations associated with material or geometric instabilities such as localisation of deformation or buckling.

In spite of these limitations, some remarkable achievements have been performed in nonlinear finite element error estimation. Between these are the developments of Ortiz and Quigley [10] in localisation, Johnson [8] in the context of the elastic-plastic model of Hencky, the error estimator of Barthold et al [4] applied to the elastic-plastic models of Hencky and Prandtl-Reuss, etc. Finally it's necessary to remark the recent works of Radovitzky and Ortiz [12] in error estimation for highly non linear problems, including finite deformations in hyperelasticity, viscoplasticity, dynamics, etc.

In what remains of this paper, the applicability of enhanced strain fields for the purpose of error estimation is explored, both for linear and nonlinear problems. The approach is based on the improved approximation qualities of enhanced assumed strain (EAS) mixed formulations such as have been proposed in [14, 16]. The error estimator may be formulated in the framework of energy norms, aiming to provide error bounds for the standard displacement finite element solutions. The formulation is developed initially for linear elasticity, and subsequently extended to finite elasticity and plasticity. Representative numerical simulations of each of these problems are presented. Although we have not found rigorous theoretical proof of the validity of our approach as an error estimator, in practice the performance of the method in the cases we have analysed is encouraging.

2. ENHANCED ASSUMED STRAIN (EAS) FINITE ELEMENT FORMULATION

The EAS finite element formulation [2, 14, 15, 16] is based on the discrete variational equations obtained from the Hu-Washizu functional [18]. The existence of a function of strain energy density is assumed, which may be expressed as a function of the linear strain tensor $\boldsymbol{\varepsilon} \equiv \varepsilon_{ij}$ for small strain problems, or the deformation gradient $\boldsymbol{F} \equiv F_{iJ}$ for finite strain problems.

The key ingredient of EAS formulations is to enrich the solution as compared to a purely displacement based formulation, using additional *assumed strain* modes. For small strains [16] the starting point is an additive decomposition of the strain field into a compatible part and an enhanced part:

$$\boldsymbol{\varepsilon} = \underbrace{\boldsymbol{\nabla}^s \boldsymbol{u}}_{\text{comp.}} + \underbrace{\widetilde{\boldsymbol{\varepsilon}}}_{\text{enh.}}; \qquad \varepsilon_{ij} = \frac{1}{2}(u_{i,j} + u_{j,i}) + \widetilde{\varepsilon}_{ij}, \tag{1}$$

where $\boldsymbol{\nabla}^s \boldsymbol{u}$ (symmetric component of the displacement gradient) is the *compatible* part of strain field, and $\widetilde{\boldsymbol{\varepsilon}}$ is the *enhanced* (or incompatible) part. This decomposition allows an *enhancement* of the numerical solution associated with the incompatible part in discrete models (for the exact continuum mechanics solution the field $\widetilde{\boldsymbol{\varepsilon}}$ would be null). There are no requirements in principle of inter-element continuity for the enhanced field $\widetilde{\boldsymbol{\varepsilon}}$, resulting in additional strain modes which are internal to each element.

For finite deformation [14, 9] EAS may be formulated in terms of displacements and deformation gradients, parametrised via the following additive decomposition:

$$\boldsymbol{F} = \underbrace{\boldsymbol{\nabla}_{\boldsymbol{X}} \boldsymbol{\varphi}}_{\text{comp.}} + \underbrace{\widetilde{\boldsymbol{F}}}_{\text{enh.}}; \qquad F_{iJ} = x_{i,J} + \widetilde{F}_{iJ}, \tag{2}$$

Prepared using nmeauth.cls

where $\boldsymbol{\varphi} : \boldsymbol{X} \mapsto \boldsymbol{x}$ is the deformation mapping, and $\boldsymbol{\nabla}_{\boldsymbol{X}}$ is the gradient with respect to the original configuration.

Full details of EAS formulations may be gathered from the above cited references, and in [6] regarding their implementation for this work.

3. ERROR ESTIMATION BASED ON ENERGY NORMS

In order to define the framework of our approach, a brief summary of concepts and notation for error estimation based on energy norms is presented below.

3.1. Variational structure of the boundary value problem

We shall consider a boundary value solid mechanics problem, for which the strong formulation is expressed in terms of the unknown displacement field $\boldsymbol{u}$ via a differential operator $\boldsymbol{A}(\boldsymbol{u})$ in $\Omega \cup \partial\Omega$:

$$\boldsymbol{A}(\boldsymbol{u}) = \boldsymbol{0} \equiv \begin{cases} \operatorname{div} \boldsymbol{\sigma} + \boldsymbol{b} = \boldsymbol{0} & \text{in } \Omega; \\ \boldsymbol{u} = \boldsymbol{g} & \text{in } \partial_g\Omega; \\ \boldsymbol{\sigma} \cdot \boldsymbol{n} = \bar{\boldsymbol{t}} & \text{in } \partial_t\Omega. \end{cases} \tag{3}$$

being $\boldsymbol{\sigma}$ the Cauchy stress tensor, $\boldsymbol{b}$ the body load per unit volume, $\boldsymbol{g}$ the imposed displacement and $\bar{\boldsymbol{t}}$ the imposed tractions. We shall further assume a variational structure of the problem, which makes (3) equivalent to minimizing the functional $\Pi(\boldsymbol{u}) = \int_\Omega W \,\mathrm{d}\Omega - \int_\Omega \boldsymbol{b}\cdot\boldsymbol{u} \,\mathrm{d}\Omega - \int_{\partial_t\Omega} \bar{\boldsymbol{t}}\cdot\boldsymbol{u} \,\mathrm{d}\Gamma$, where $W = W(\boldsymbol{\varepsilon}(\boldsymbol{u}), \boldsymbol{x})$ is the function of strain energy density, $\boldsymbol{b}$ the volume forces and $\bar{\boldsymbol{t}}$ the applied surface tractions.

The Dirichlet form $a(\boldsymbol{u})[\delta\boldsymbol{u}, \delta\boldsymbol{u}]$ associated with the strain energy is defined as the second variation of the functional. Defining the tangent elastic moduli $\boldsymbol{D} = \partial^2 W/\partial\boldsymbol{\varepsilon}\partial\boldsymbol{\varepsilon}$, it is expressed as

$$a(\boldsymbol{u})[\delta\boldsymbol{u}, \delta\boldsymbol{u}] = \int_\Omega \boldsymbol{\nabla}_{\boldsymbol{x}}\delta\boldsymbol{u} \cdot \left(\boldsymbol{D} \cdot \boldsymbol{\nabla}_{\boldsymbol{x}}\delta\boldsymbol{u}\right) \mathrm{d}\Omega = \int_\Omega D_{ijkl}\delta u_{i,j}\delta u_{k,l} \mathrm{d}\Omega \tag{4}$$

where sums on repeated indices are understood, and $\delta\boldsymbol{u} \in \mathcal{V}$ are admissible variations within the space of functions with finite energy norm, satisfying homogeneous kinematic boundary conditions in $\partial_g\Omega$.

For the particular case of linear elasticity $\boldsymbol{D}$ does not depend on $\boldsymbol{u}$, and application of (4) to the displacement field $\boldsymbol{u}$ itself yields twice the strain energy, $a[\boldsymbol{u}, \boldsymbol{u}] = \int_\Omega \boldsymbol{\varepsilon} \cdot (\boldsymbol{D} \cdot \boldsymbol{\varepsilon}) \,\mathrm{d}\Omega = 2\int_\Omega W \,\mathrm{d}\Omega$. In a general case, the *energy norm* for a given field $\boldsymbol{v}$ is defined as

$$\|\boldsymbol{v}\|_E \stackrel{\text{def}}{=} a(\boldsymbol{u})[\boldsymbol{v}, \boldsymbol{v}]^{\frac{1}{2}}. \tag{5}$$

The form $a(\boldsymbol{u})[\delta\boldsymbol{u}, \delta\boldsymbol{u}]$ is *regular* if 1) the coefficients $\boldsymbol{D} \equiv D_{ijkl}$ are bounded in Ω, and 2) there exists $C \in \mathbb{R}^+$ such that $a(\boldsymbol{u})[\delta\boldsymbol{u}, \delta\boldsymbol{u}]^{\frac{1}{2}} > C\|\delta\boldsymbol{u}\|_1$, where $\|\delta\boldsymbol{u}\|_1 \stackrel{\text{def}}{=} \left[\sum_{\alpha=0}^{1} \int_\Omega (\mathrm{D}^\alpha\delta\boldsymbol{u})^2 \,\mathrm{d}\Omega\right]^{\frac{1}{2}}$ (1st. Sobolev norm). Under these circumstances the functional $\Pi(\boldsymbol{u})$ is convex and has a unique relative minimum. Hence, the solution $\boldsymbol{u}$ of the boundary value problem verifies:

$$\Pi(\boldsymbol{u}) = \inf_{\boldsymbol{v}\in V} \Pi(\boldsymbol{v}). \tag{6}$$

The variational equation associated with the functional $\Pi(\boldsymbol{u})$ is:

$$G(\boldsymbol{u})[\delta\boldsymbol{u}] = 0 \quad \forall \delta\boldsymbol{u} \in \mathcal{V}. \tag{7}$$

where $G(\boldsymbol{u})[\delta\boldsymbol{u}]$ is the weak form derived from the boundary value problem (3). Following we shall restrict ourselves to the case of linear elasticity,

$$G(\boldsymbol{u})[\delta\boldsymbol{u}] = -\int_\Omega \boldsymbol{\sigma} \cdot \boldsymbol{\nabla}_{\boldsymbol{x}}(\delta\boldsymbol{u})\,\mathrm{d}\Omega + \int_\Omega \boldsymbol{b}\cdot\delta\boldsymbol{u}\,\mathrm{d}\Omega + \int_{\partial_t\Omega} \overline{\boldsymbol{t}}\cdot\delta\boldsymbol{u}\,\mathrm{d}\Gamma \tag{8}$$

Let us now consider the following two expressions: firstly, the restriction of (8) to variations $\delta\boldsymbol{u}_h \in \mathcal{V}_h$,

$$G(\boldsymbol{u})[\delta\boldsymbol{u}_h] = 0 \quad \forall \delta\boldsymbol{u}_h \in \mathcal{V}_h; \tag{9}$$

and second, the particularisation of (8) to $\boldsymbol{u}_h \in \mathcal{V}_h$,

$$G(\boldsymbol{u}_h)[\delta\boldsymbol{u}_h] = 0 \quad \forall \delta\boldsymbol{u}_h \in \mathcal{V}_h. \tag{10}$$

Subtracting these two equations, taking into account the linearity of $G(\boldsymbol{u})[\delta\boldsymbol{u}]$, the following result is obtained, expressed in terms of the Dirichlet form:

$$a(\boldsymbol{u})[\boldsymbol{u}-\boldsymbol{u}_h, \delta\boldsymbol{u}_h] = 0 \quad \forall \delta\boldsymbol{u}_h \in \mathcal{V}_h \tag{11}$$

Equation (11) indicates that the finite element solution minimises the value of the energy norm $\|\boldsymbol{u}-\boldsymbol{u}_h\|_E$. This property is referred to as the *optimal approximation property* of the finite element method:

$$\|\boldsymbol{u}-\boldsymbol{u}_h\|_E = \inf_{\boldsymbol{v}_h\in\mathcal{V}_h} \|\boldsymbol{u}-\boldsymbol{v}_h\|_E. \tag{12}$$

3.2. Local error estimation

In general, the finite element solution is obtained in the discretised domain Ω^h, which is constructed via the discretisation of the body $\Omega \subset \mathbb{R}^3$ in n_{el} elements Ω^e, $e = 1, \dots n_{\mathrm{el}}$.

Let the finite energy function $\boldsymbol{u}^e$ be the exact displacement field in Ω^e. The *finite dimension interpolant polynomial* of the exact solution $\boldsymbol{u}^e$ is:

$$\boldsymbol{u}_h^e(\boldsymbol{x}) \stackrel{\mathrm{def}}{=} \sum_{a=1}^{n_{\mathrm{nen}}} \boldsymbol{u}_a N_a(\boldsymbol{x}) \in \mathbb{P}_k(\Omega^e) \tag{13}$$

being n_{nen} the number of nodes of element e, and $\mathbb{P}_k(\Omega^e)$ the set of polynomials over Ω^e with degree lower or equal than k.

The local error function in element Ω_e is defined in each point as the difference between the exact displacement field and the approximate displacement field computed via the finite element method:

$$\boldsymbol{E}^e(\boldsymbol{x}) = \boldsymbol{u}^e(\boldsymbol{x}) - \boldsymbol{u}_h^e(\boldsymbol{x}) \tag{14}$$

The objective of the local error estimator is to obtain an upper bound of the local error function (14), which may be expressed as:

$$\|\boldsymbol{u}^e - \boldsymbol{u}_h^e\|_E \leq C(h^e)^\alpha |\boldsymbol{u}^e| \tag{15}$$

where $C > 0$ is constant, h^e the diameter of Ω^e, $|\boldsymbol{u}^e|$ a seminorm of $\boldsymbol{u}^e$ and α the rate of convergence. The inequality (15) is verified if the *optimal approximation property* (12) and the regularity conditions for $a(\boldsymbol{u})[\cdot,\cdot]$ hold [5].

3.3. Global error estimation

Since $\|\boldsymbol{u}_e^h\|_E$ is bounded, if the shape functions in (13) are conforming, then the global interpolant function defined as $\boldsymbol{u}_h = \sum_{e=1}^{n_{\text{el}}} \boldsymbol{u}_h^e$ is also a finite energy function. In such situation, the upper bound of the global error function expressed in (15) can be obtained as the sum of the element contributions. Performing this sum, if the regularity conditions hold, the inequality (15) results in:

$$\|\boldsymbol{u} - \boldsymbol{u}_h\|_E \leq C \sum_{e=1}^{n_{\text{el}}} \frac{(h^e)^{k+1}}{\rho^e} |\boldsymbol{u}|_{k+1} \tag{16}$$

where $|\boldsymbol{u}|_{k+1}$ is the $(k+1)$st. Sobolev seminorm, $|\boldsymbol{u}|_{k+1} = \left[\int_\Omega (\mathrm{D}^{k+1}\boldsymbol{u})^2 \, \mathrm{d}\Omega\right]^{\frac{1}{2}}$, and ρ^e is the diameter of the largest sphere in Ω_e.

4. ERROR ESTIMATOR PROPOSED

From a practical point of view, equation (16) is not convenient because the error is expressed in terms of the a priori unknown exact solution $\boldsymbol{u}^e$. Further it is not possible to substitute this field by its approximate solution $\boldsymbol{u}_h^e$, as it is a polynomial of degree k and the seminorm used is of order $k+1$ ($\mathrm{D}^{k+1}\boldsymbol{u}_h^e = 0$).

Our objective is to build an error estimator for the approximate solution, calculated with (compatible) displacement elements. For this the finite element solution $\boldsymbol{u}_{\text{enh}}$ obtained with the EAS elements described in section 2 will be used. The starting point is the triangular inequality for the energy norm as follows:

$$\|\boldsymbol{u} - \boldsymbol{u}_h\|_E \leq \|\boldsymbol{u} - \boldsymbol{u}_{\text{enh}}\|_E + \|\boldsymbol{u}_{\text{enh}} - \boldsymbol{u}_h\|_E \tag{17}$$

Assuming both finite element solutions are convergent, we can express

$$\|\boldsymbol{u} - \boldsymbol{u}_{\text{enh}}\|_E = \mathcal{O}(h^m) \tag{18}$$

$$\|\boldsymbol{u}_{\text{enh}} - \boldsymbol{u}_h\|_E = \mathcal{O}(h^p) \tag{19}$$

A key assumption we shall now make is that, at least in the asymptotic regime ($h \to 0$), the rates of convergence in the above expressions are as follows:

$$\boxed{m > p} \tag{20}$$

In these conditions, as the mesh is refined, the first term on the right hand side of equation (17) becomes negligible as compared to the second one. Therefore it is possible to establish that:

$$\|\boldsymbol{u} - \boldsymbol{u}_h\|_E \leq C \|\boldsymbol{u}_{\text{enh}} - \boldsymbol{u}_h\|_E, \quad C \in \mathbb{R}^+ \tag{21}$$

Hypotheses (18, 19, 20) may be interpreted plainly in the following terms: it is assumed that both the enhanced solution $\boldsymbol{u}_{\text{enh}}$ and the displacement solution $\boldsymbol{u}_h$ converge to the exact solution, in such manner that

1. Their difference, measured by the energy norm $\|\boldsymbol{u}_{\text{enh}} - \boldsymbol{u}_h\|_E$, decreases with mesh refinement;

2. The difference between the solution with EAS and the exact solution decreases faster (with increasing number the elements) than the difference between the solution with EAS and the standard displacement formulation.

The second statement is true if compatible finite element formulation exhibits locking, e.g. incompressible elasticity, dominated bending situations, etc. Otherwise (compressible elasticity without significant bending, mild locking, etc.) it is not possible to judge in advance if (20) is verified. We have not found a rigorous proof of the general validity of this hypothesis. However, in the practical applications we have performed some of which are included further down in this paper, it has been fount to be valid.

As a consequence, the local error estimator proposed is the energy norm of the difference between the enhanced and the displacement solutions:

$$\boxed{(E^e)^2 = \|\boldsymbol{u}^e_{\text{enh}} - \boldsymbol{u}^e_h\|_E} \tag{22}$$

As discussed in subsection 3.3, the global error may then be obtained as the sum of the local errors:

$$E^2 = \sum_{e=1}^{n_{\text{el}}} (E^e)^2 \tag{23}$$

In summary, in order to compute the local error estimator (22), the discretisation error associated with the standard elements is quantified via the energy norm associated with the incompatible modes computed with enhanced elements.

Each component in the sum (23) is local. Therefore the proposed estimator has the advantage that it is computed element by element, without recourse to global smoothing techniques nor sub-domain solutions apart from the computation of the enhanced strain field.

5. ERROR ESTIMATION IN FINITE ELASTICITY PROBLEMS

The error estimator proposed above may be generalised for finite elasticity problems with hyperelastic models. Here the unknown field shall be the deformation mapping $\boldsymbol{\varphi} : \Omega \ni \boldsymbol{X} \mapsto \boldsymbol{x} \in \Omega_t$, where Ω is the reference configuration and Ω_t is the deformed configuration at time t. The basis of this formulation is similar to that described in section 3, replacing here the displacement field $\boldsymbol{u}$ by the deformation mapping $\boldsymbol{\varphi}$, and the linear strain tensor $\boldsymbol{\varepsilon}$ by the deformation gradient $\boldsymbol{F} = \boldsymbol{\nabla}_{\boldsymbol{X}} \boldsymbol{\varphi}$.

With respect to the approximation methodology the following result is obtained in a similar way to equation (11):

$$G(\boldsymbol{\varphi})[\delta\boldsymbol{\varphi}_h] - G(\boldsymbol{\varphi}_h)[\delta\boldsymbol{\varphi}_h] = 0 \quad \forall \delta\boldsymbol{\varphi}_h \in \mathcal{V}_h \tag{24}$$

In this case it's not possible to group the two terms in (24), leading to a expression similar to (11), because in finite elasticity the weak form $G(\boldsymbol{\varphi})[\delta\boldsymbol{\varphi}]$ is *nonlinear* in $\boldsymbol{\varphi}$. However, considering the asymptotic regime ($h \to 0$), the finite element solution $\boldsymbol{\varphi}_h$ will approach the exact solution; as $(\boldsymbol{\varphi} - \boldsymbol{\varphi}_h) \to \boldsymbol{0}$, equation (24) may be linearised, resulting in:

$$G(\boldsymbol{\varphi})[\delta\boldsymbol{\varphi}_h] - G(\boldsymbol{\varphi}_h)[\delta\boldsymbol{\varphi}_h] \approx a(\boldsymbol{\varphi})[\boldsymbol{\varphi} - \boldsymbol{\varphi}_h, \delta\boldsymbol{\varphi}_h] = 0 \quad \forall \delta\boldsymbol{\varphi}_h \in \mathcal{V}_h, \quad h \to 0 \tag{25}$$

This condition establishes the *optimal approximation property* of the finite element method for finite elasticity, in the asymptotic regime [12]:

$$\|\boldsymbol{\varphi} - \boldsymbol{\varphi}_h\|_E = \inf_{\boldsymbol{v_h} \in \mathcal{V}_h} \|\boldsymbol{\varphi} - \boldsymbol{v}_h\|_E \qquad h \to 0 \tag{26}$$

For finite deformations, the equivalent assumptions to (18, 19) are expressed now in terms of the deformation mapping $\boldsymbol{\varphi}$:

$$\|\boldsymbol{\varphi} - \boldsymbol{\varphi}_{\text{enh}}\|_E = \mathcal{O}(h^m) \tag{27}$$

$$\|\boldsymbol{\varphi}_{\text{enh}} - \boldsymbol{\varphi}_h\|_E = \mathcal{O}(h^p) \tag{28}$$

$$m > p \tag{29}$$

Then, if (27, 28, 29) are verified, the expression of the local error estimator proposed in (22) results in:

$$\boxed{(E^e)^2 = \|\boldsymbol{\varphi}^e_{\text{enh}} - \boldsymbol{\varphi}^e_h\|_E} \tag{30}$$

For numerical implementation, the value of (30) is computed in the reference configuration. The expression of the energy norm, for a given field value $\boldsymbol{\eta}$, is [5]:

$$(\|\boldsymbol{\eta}\|_E)^2 = a(\boldsymbol{\varphi})[\boldsymbol{\eta}, \boldsymbol{\eta}] = \int_\Omega \boldsymbol{\nabla_x \eta} \cdot (\boldsymbol{D} \cdot \boldsymbol{\nabla_x \eta})\, \mathrm{d}\Omega \tag{31}$$

where $\boldsymbol{D}$ is the tangent tensor of constitutive moduli:

$$\boldsymbol{D} = \frac{\partial^2 W(\boldsymbol{X}, \boldsymbol{F})}{\partial \boldsymbol{F} \partial \boldsymbol{F}} \tag{32}$$

Straightforward calculations in (30) taking into account (2) provide the closed form of the error estimator [6]:

$$(E^e)^2 = \frac{1}{2} \int_{\Omega^e} \widetilde{\boldsymbol{F}} \cdot (\boldsymbol{D} \cdot \widetilde{\boldsymbol{F}})\, \mathrm{d}\Omega \tag{33}$$

being $\widetilde{\boldsymbol{F}}$ the enhanced part of the deformation gradient (2). Note that expression (33) is configuration dependent, as moduli $\boldsymbol{D}$ change. Computing the global error via (33) extended over the complete domain Ω, it can be expressed as the sum of the local errors:

$$E^2 = \sum_{e=1}^{n_{\text{el}}} (E^e)^2 \tag{34}$$

6. ERROR ESTIMATION IN VON MISES PLASTICITY

The methodology of error estimation discussed in section 4 and generalised to finite elasticity problems in section 5, is now further extended to elastic-plastic small strain problems, with Von Mises yield criterion. The methodology described above assumes a variational structure of the boundary value problem. In plasticity, this variational structure may be obtained at an incremental level via the variational integration of the plasticity equations [11]. This variational

integration postulates the existence of an incremental energy function per unit volume $W_{t+\Delta t}$, for solving step $t+\Delta t$ from the results in step t, such that

$$\boldsymbol{\sigma}_{t+\Delta t} = \frac{\partial W_{t+\Delta t}}{\partial \boldsymbol{\varepsilon}^e_{t+\Delta t}} \tag{35}$$

where $\boldsymbol{\varepsilon}^e_{t+\Delta t}$ are the elastic strains at time $t+\Delta t$.

A general formulation for finite deformation plasticity in dynamic regime has been developed by Radovitzky and Ortiz [12]. We follow this same approach, particularising it for small strain J_2 plasticity with isotropic hardening. The functional dependence of $W_{t+\Delta t}$ is on elastic strain and effective plastic strain $\xi = \int_0^t 2/3\,(\dot{\boldsymbol{\varepsilon}}^p \cdot \dot{\boldsymbol{\varepsilon}}^p)^{1/2}\,\mathrm{d}t$. The expression of the incremental potential function is [11]:

$$W_{t+\Delta t}(\boldsymbol{\varepsilon}^e_{t+\Delta t}, \xi_{t+\Delta t}, \boldsymbol{\varepsilon}^e_t, \xi_t) = \min_{\xi_{t+\Delta t}} \left(\Psi_{t+\Delta t}(\boldsymbol{\varepsilon}^e_{t+\Delta t}, \xi_{t+\Delta t}) - \Psi_t(\boldsymbol{\varepsilon}^e_t, \xi_t)\right) \tag{36}$$

where $\Psi(\boldsymbol{\varepsilon}^e, \xi)$ is the free energy function. The requirement for a minimum in the right-hand side of (36) is equivalent to the condition:

$$\frac{\partial \Psi_{t+\Delta t}(\boldsymbol{\varepsilon}^e_{t+\Delta t}, \xi_{t+\Delta t})}{\partial \xi_{t+\Delta t}} = 0 \tag{37}$$

Assuming that the elastic response is independent of the phenomena associated with unrecoverable distortions of the crystalline lattice, the free energy function may be expressed via the additive decomposition in an elastic part and a plastic part. Besides, if the additive decomposition of the infinitesimal strain tensor is assumed:

$$\Psi(\boldsymbol{\varepsilon}^e, \xi) = \Psi^e(\boldsymbol{\varepsilon}^e) + \Psi^p(\xi); \qquad \boldsymbol{\varepsilon} = \boldsymbol{\varepsilon}^e + \boldsymbol{\varepsilon}^p, \tag{38}$$

the incremental potential $W_{t+\Delta t}$ in (36) can be written as:

$$W_{t+\Delta t} = \min_{\xi_{t+\Delta t}} \left(\Psi^e_{t+\Delta t}(\boldsymbol{\varepsilon}_{t+\Delta t} - \boldsymbol{\varepsilon}^p_{t+\Delta t}) + \Psi^p_{t+\Delta t}(\xi_{t+\Delta t}) - \Psi^e_t(\boldsymbol{\varepsilon}_t - \boldsymbol{\varepsilon}^p_t) - \Psi^p_t(\xi_t)\right) \tag{39}$$

The optimisation condition (37) applied to (39), leads to the following expression [6]:

$$\left(J_{2,_{t+\Delta t}}\right)^2 = \frac{2}{3}\frac{\partial \Psi^p}{\partial \xi_{t+\Delta t}} \tag{40}$$

where J_2 is the second invariant of the deviatoric part of the Cauchy stress tensor. In this situation the boundary value problem is described via an incremental differential operator, $\boldsymbol{A}_{t+\Delta t}(\boldsymbol{u}) = \boldsymbol{0}$. The corresponding Dirichlet form is

$$a(\boldsymbol{u}_{t+\Delta t})[\delta\boldsymbol{u}, \delta\boldsymbol{u}] = \int_\Omega \boldsymbol{\nabla}^{\mathrm{s}}(\delta\boldsymbol{u}) \cdot \left(\frac{\partial^2 W_{t+\Delta t}}{\partial \boldsymbol{\varepsilon}_{t+\Delta t} \partial \boldsymbol{\varepsilon}_{t+\Delta t}} \cdot \boldsymbol{\nabla}^{\mathrm{s}}(\delta\boldsymbol{u})\right) \mathrm{d}\Omega \tag{41}$$

If (41) verifies the regularity conditions, the error estimation methodology described in previous sections is applicable. Then, the local error estimator for this kind of problems is:

$$\boxed{(E^e_{\Delta t})^2 = \|\boldsymbol{u}^e_{\mathrm{enh}_{t+\Delta t}} - \boldsymbol{u}^e_{h_{t+\Delta t}}\|_E} \tag{42}$$

The error bound proposed in (42) is an incremental bound of absolute error in a given time-step Δt. In order to evaluate the discretisation error along the complete load path, it is necessary to determine the integral of $E^e_{\Delta t}$ over time:

$$(E^e_{t+\Delta t})^2 = \int_0^{t+\Delta t} (E^e_{\Delta t})^2 \mathrm{d}t \tag{43}$$

The above expression indicates that accumulation of the error is performed by summing the squares. This causes one of the limitations of this error estimator as a global measure for the complete load path: it is computed as an increasing monotonic function, as the integrand is always positive. It will not reflect correctly situations in which errors may tend to reduce locally along a complex load path or bifurcations.

Using the incremental function $W_{t+\Delta t}$, the error estimator is interpreted as the contribution of the incompatible modes of the free energy function:

$$(E^e_{\Delta t})^2 = \int_{\Omega_e} W_{t+\Delta t} \left(\boldsymbol{\varepsilon}^e_{t+\Delta t} - \boldsymbol{\varepsilon}^e_{t+\Delta t}(\boldsymbol{u}), \xi_{t+\Delta t} - \xi_{t+\Delta t}(\boldsymbol{u}), \boldsymbol{\varepsilon}^e_t - \boldsymbol{\varepsilon}^e_t(\boldsymbol{u}), \xi_t - \xi_t(\boldsymbol{u})\right) \mathrm{d}\Omega \tag{44}$$

The energy density in (44) can be decomposed additively with the contributions of the elastic and plastic part of the free energy, resulting in:

$$\begin{aligned}(E^e_{\Delta t})^2 = &\int_{\Omega_e} W^e_{t+\Delta t} \left(\boldsymbol{\varepsilon}^e_{t+\Delta t} - \boldsymbol{\varepsilon}^e_{t+\Delta t}(\boldsymbol{u}), \boldsymbol{\varepsilon}^e_t - \boldsymbol{\varepsilon}^e_t(\boldsymbol{u})\right) \mathrm{d}\Omega + \\ &\int_{\Omega_e} W^p_{t+\Delta t} \left(\xi_{t+\Delta t} - \xi_{t+\Delta t}(\boldsymbol{u}), \xi_t - \xi_t(\boldsymbol{u})\right) \mathrm{d}\Omega\end{aligned} \tag{45}$$

The global discretisation error is obtained extending the integral in (44) to the complete domain Ω. Then, the global error is computed via the summation of the local errors:

$$E^2_{\Delta t} = \sum_{i=1}^{n_{\mathrm{el}}} (E^i_{\Delta t})^2 \tag{46}$$

7. NUMERICAL SIMULATIONS

7.1. 3-D linear elasticity. Scordelis-Lo roof

The classical Scordelis-Lo test for shell elements [13], is solved here with 3D solid elements in order to show the behaviour of the error estimator using an isotropic linear elasticity model. On an 80° cylindrical sector roof a volumetric load is acting in Z direction. The roof is supported on two rigid diaphragms. Figure 1 shows the problem definition taking into account the symmetry conditions. The numerical values of the elastic constants are [13]: $E = 4.32 \cdot 10^8$, $\nu = 0$, and the dimensions of the roof are $L = 50$, $R = 25$, $t = 0.25$ and $b = 360$.

The results obtained with enhanced assumed strain elements are very adequate for error estimation because they approach closely those obtained with shell elements, as shown in table I for several meshes with only one element across the thickness. The results for shell elements referenced in this table have been obtained with the four node general purpose thick

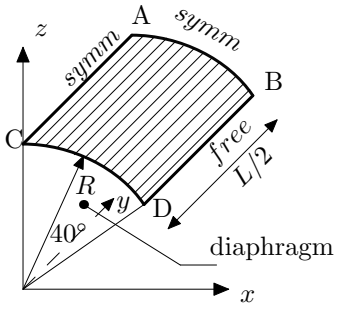

Figure 1. *Scordelis-Lo roof. Definition of the problem.*

Table I. *Results obtained with 3D enhanced elements and thick shell elements for Scordelis-Lo test*

N° of elements	v_B (solid elements)	v_B (shell elements)
$4 \times 4 \times 1$	0.1656	0.3132
$8 \times 8 \times 1$	0.2896	0.3031
$16 \times 16 \times 1$	0.3031	0.3016
$32 \times 32 \times 1$	0.3038	0.3016
$64 \times 64 \times 1$	0.3042	0.3018

shell element S4 from a commercial program element library [1]. The vertical displacement of point B computed with $16 \times 16 \times 1$ enhanced solid elements is $v_B = 0.3031$, very similar to the result $v_{\text{ref}} = 0.3024$ reported in the literature [13].

For error estimation the exact solution adopted here is obtained with a 24961 D.O.F. reference mesh, solved with enhanced assumed strain elements. The error estimation is analysed refining over the surface of the roof with only one element along the thickness, as well as refining through the thickness. The meshes considered for the first case are those referenced in table I. The meshes used for refinement along the thickness are $16 \times 16 \times 1$, $16 \times 16 \times 2$, $16 \times 16 \times 3$, $16 \times 16 \times 4$, $16 \times 16 \times 5$ and $16 \times 16 \times 10$.

Figure 2 shows the energy norm $\|\boldsymbol{u}_{\text{ref}}\|_E$ computed with the reference mesh, the energy norm computed with enhanced elements $\|\boldsymbol{u}_{\text{enh}}\|_E$, and the energy norm computed with standard displacement elements $\|\boldsymbol{u}_{\text{h}}\|_E$ versus the number of degrees of freedom, for refinement over the surface. The refinement across the thickness does not show a significant influence on the energy norm [7]. Figures 3 and 4 show the evolution of the global error estimated in terms of the number of degrees of freedom. The theoretical error is evaluated as the difference between the reference energy norm and the energy norm computed with standard elements.

In order to check the assesment of the key hypothesis (20) the rates of convergence m and p employed in the said hypothesis have been computed. The exponent m in $\|\boldsymbol{u} - \boldsymbol{u}_h\|_E = Ch^m$ is approximated via the difference of the reference mesh norm $\|\boldsymbol{u}_{\text{ref}}\|_E$ minus $\|\boldsymbol{u}_h\|_E$ and the exponent p in $\|\boldsymbol{u}_{\text{enh}} - \boldsymbol{u}_h\|_E = Ch^p$ is obtained directly from the finite element computation of the error estimator. Each value of m and p is obtained from the results of two meshes with parameters h_1 and h_2, and the assumption that C and the rate of convergence (m or p)

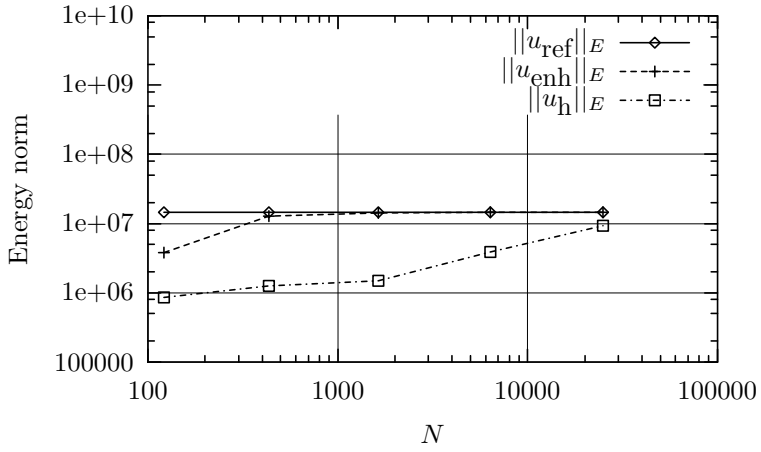

Figure 2. *Variation of energy norm with no. of D.O.F. for refinement over the surface*

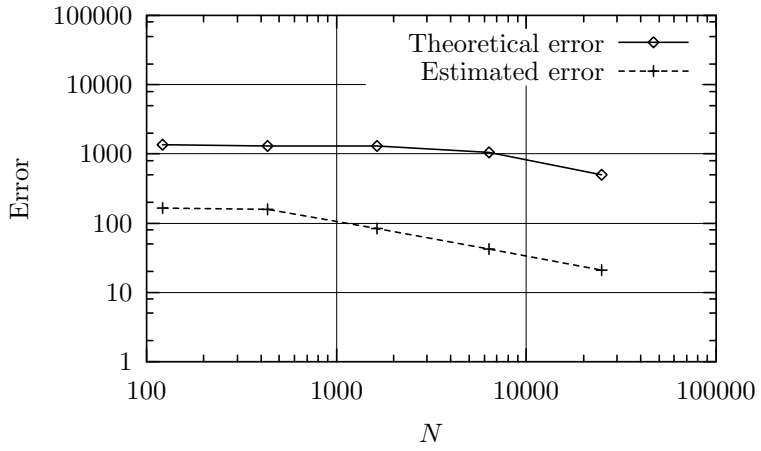

Figure 3. *Evolution of global error with respect to no. of D.O.F. for refinement over the surface*

are constant for the two meshes (in a similar way to Richardson's extrapolation). In table II the values obtained for m and p in the Scordelis-Lo test are shown. For all the meshes the hypothesis expressed in (20) is fount to be valid. Finally, figure 5 shows the error contours obtained with two of the considered meshes.

7.2. 2-D Finite elasticity. Double notched specimen

This test has been proposed for error estimation by Radovitzky and Ortiz [12]. A double notched specimen in plain strain is considered in mode I crack opening. The analysis is carried out with displacement control. The hyperelastic constitutive model has the following energy function:

$$W(\boldsymbol{C}) = \frac{1}{2}\lambda(\log J)^2 - \mu \log(J) + \frac{1}{2}\mu(\text{trace}(\boldsymbol{C}) - 3) \tag{47}$$

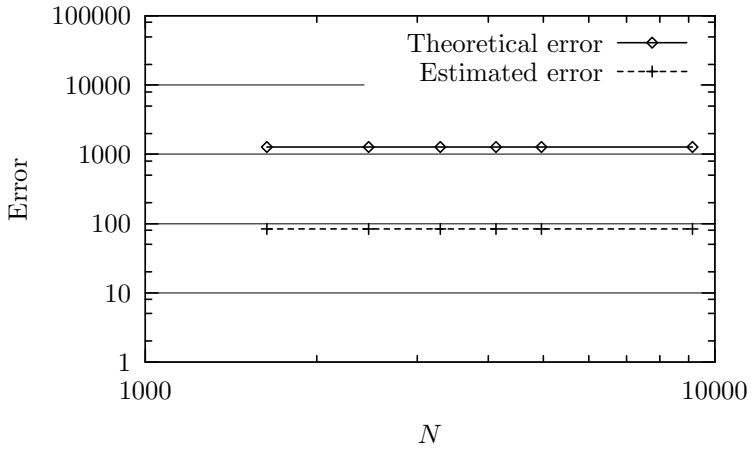

Figure 4. *Evolution of global error with no. of D.O.F. for refinement along thickness*

Table II. *Computed values of the rates of convergence m and p in hypothesis (20) for Scordelis-Lo test*

Mesh parameter	m	p
h		
	1.3656	0.0646
$h/2$		
	1.7541	0.9171
$h/4$		
	1.9035	0.9940
$h/8$		

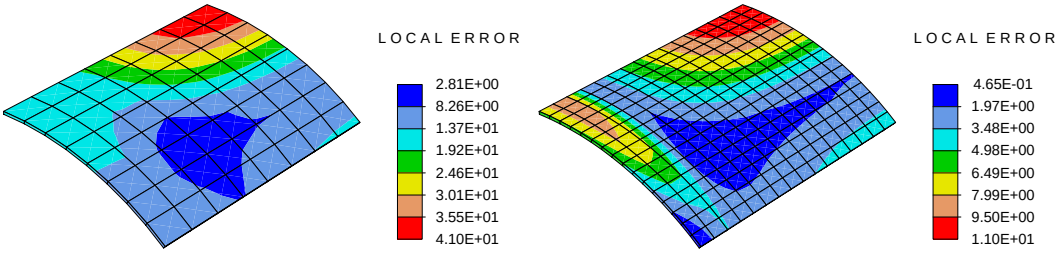

Figure 5. *Scordelis roof. Contours of iso-error computed for the* $8 \times 8 \times 1$ *and* $16 \times 16 \times 1$ *meshes*

with $\boldsymbol{C} = \boldsymbol{F}^T \boldsymbol{F}$ (right Cauchy tensor), $J = \det(\boldsymbol{F})$ and (λ, μ) the Lamé elastic moduli. The values adopted for these constants are: $\lambda = 110.74$ and $\mu = 80.194$. Six meshes have been considered with 16, 64, 256, 1024, 4096 and 6400 elements with uniform remeshing. The last one is considered in order to obtain a reference value for the energy norm $\|\boldsymbol{\varphi}_{\text{ref}}\|_E$.

Figure 6 shows the contours of local error for the meshes with 16 and 64 elements. These

contours are drawn over the deformed mesh (without magnification) in order to show the finite strains reached (lips of the notch were initially in touch). As expected, the discretisation error is concentrated near the tip of the crack.

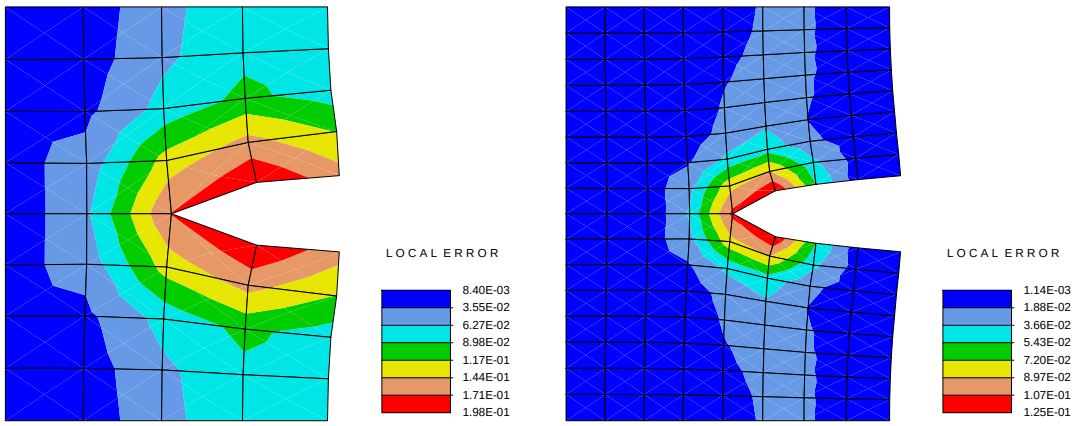

Figure 6. *Double notched specimen. Contours of iso-error for* 16 *and* 64 *elements meshes*

Figure 7 shows the energy norms $\|\boldsymbol{\varphi}_{\rm ref}\|_E$, $\|\boldsymbol{\varphi}_{\rm enh}\|_E$ and $\|\boldsymbol{\varphi}_{\rm h}\|_E$, computed with the reference mesh, enhanced elements and standard displacement elements, respectively, versus the number of degrees of freedom. Figure 8 shows the global estimated error ($\|\boldsymbol{\varphi}_{\rm enh} - \boldsymbol{\varphi}_{\rm h}\|_E$) and the global theoretical error computed as difference of norms $\|\boldsymbol{\varphi}_{\rm ref}\|_E - \|\boldsymbol{\varphi}_{\rm h}\|_E$, versus N (number of D.O.F.s).

From these figures it is concluded that the error estimator is convergent and it agrees with the theoretical error. Besides, the assesment of hypothesis (29) shows it to be valid in this example too. To this end, the methodology followed is the same as in the previous example. Table III shows the values obtained for m and p. Although initially for the coarse meshes $m < p$, thus not verifying (29), after some refinements $m > p$ proves to be valid.

7.3. Plasticity. Square plate with circular hole

This final example simulates the tensile test of a square plate with a circular hole under plane strain conditions. It has been used as benchmark test for error estimation in [17]. A summary of the results obtained has been published in [4]. There are two singular points in the diameter normal to the direction of the imposed displacements. The layout and boundary conditions are shown in figure 9, where $l = 50$ and $r = 10$, and $u = 0.32$ is the final value of the prescribed displacement. The constitutive behaviour is modelled with an elastic-plastic Von Mises model with the following saturation law for hardening:

$$\sigma_Y = \sigma_0 + (\sigma_\infty - \sigma_0)(1 - e^{-\beta\xi}) + H\xi \tag{48}$$

The numerical values adopted are: $\sigma_0 = 450$, $\sigma_\infty = 750$, $\beta = 16.93$, $H = 129$. The elastic behaviour is defined with elastic moduli $E = 206900$ and $\nu = 0.29$. For the error estimation four meshes with 37, 407, 1583 and 3119 degrees of freedom are considered.

Table III. *Computed values of the rates of convergence m and p in hypothesis (29) for Double Notched Specimen test*

Mesh parameter	m	p
h		
	0.3658	0.7952
$h/2$		
	0.5648	0.6832
$h/4$		
	0.6209	0.5727
$h/8$		
	0.7356	0.6659
$h/16$		
	1.3355	0.7189
$h/32$		

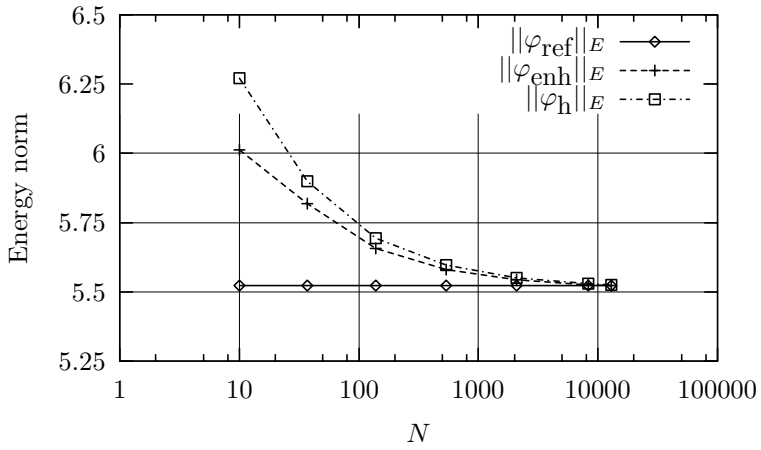

Figure 7. *Double notched specimen. Variation of energy norm versus no. of D.O.F.*

Figure 10 shows the global error estimated at the end of the computation, with respect to the number of degrees of freedom. The values of the error estimator obtained predict a low order of convergence: the 1/8 slope plotted in double logarithmic scale is well adjusted to the rate of convergence obtained in the computations.

Figure 11 shows the local error contours at the end of the process. These values are obtained adding along the load path the incremental values obtained via (44). The maximum values of contours are reached in the singular point, and as the mesh is refined the contours are localised in a 45° band.

Finally the evolution of the local error near the singular point is studied. The error is decomposed additively into an elastic and a plastic part, in accordance to (45). The two components are shown in figure 12 and 13, respectively. The conclusions obtained from these curves are:

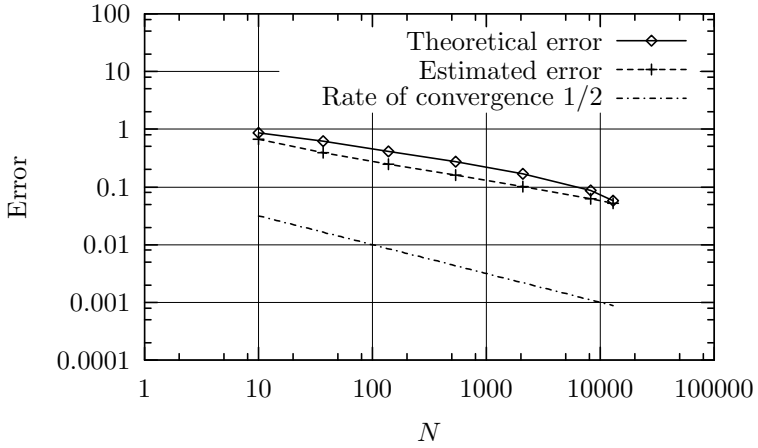

Figure 8. *Double notched specimen. Variation of error versus D.O.F.*

1. The elastic and plastic parts of the local error decrease with mesh refinement, although the plastic part is activated earlier in the refined meshes.
2. Both components of the error increase along the load process
3. The order of magnitude of both components is similar.

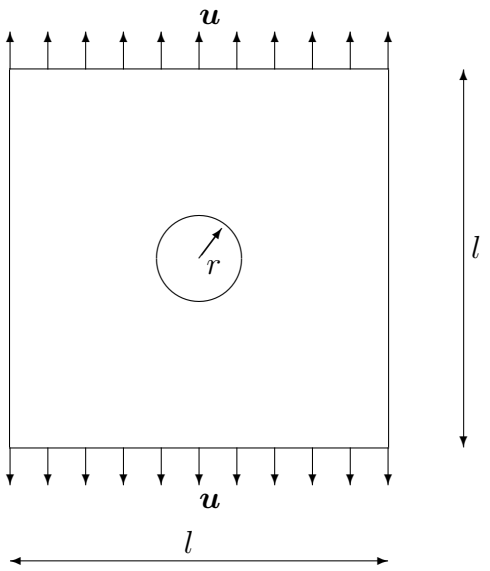

Figure 9. Square plate with circular hole. Geometry and boundary conditions

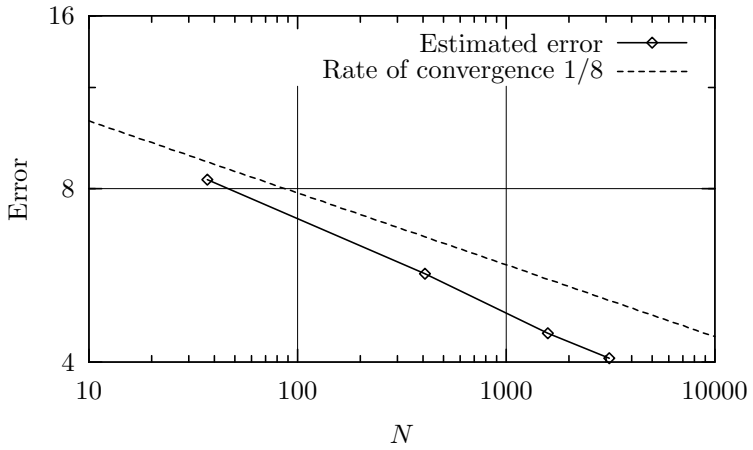

Figure 10. *Square plate with circular hole. Global error estimated*

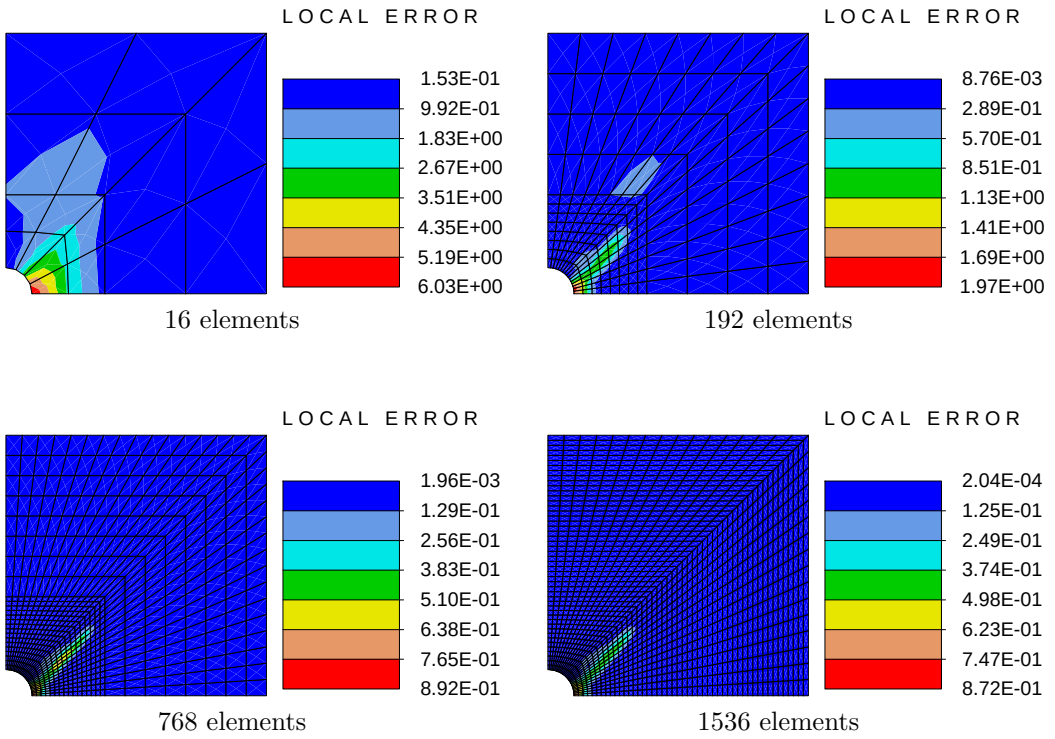

Figure 11. *Square plate with circular hole. Contours of local error*

8. CONCLUDING REMARKS

The application of enhanced strain fields for error estimation in non linear problems has been discussed. The error estimator proposed is based on the energy norm contribution of

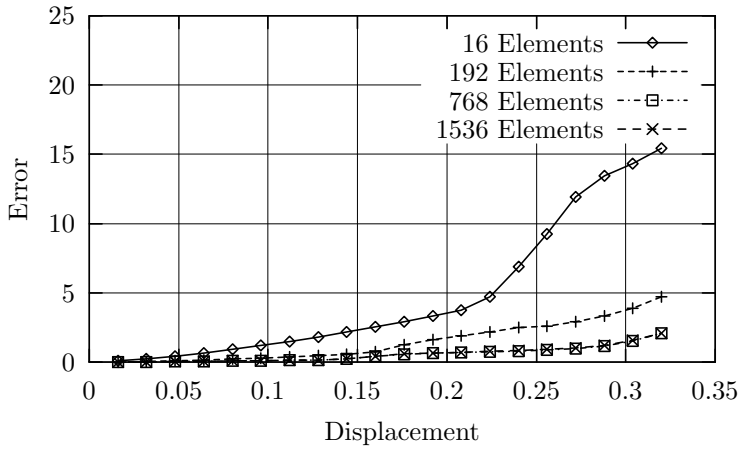

Figure 12. *Square plate with a hole. Evolution of the elastic part of local error near the singular point.*

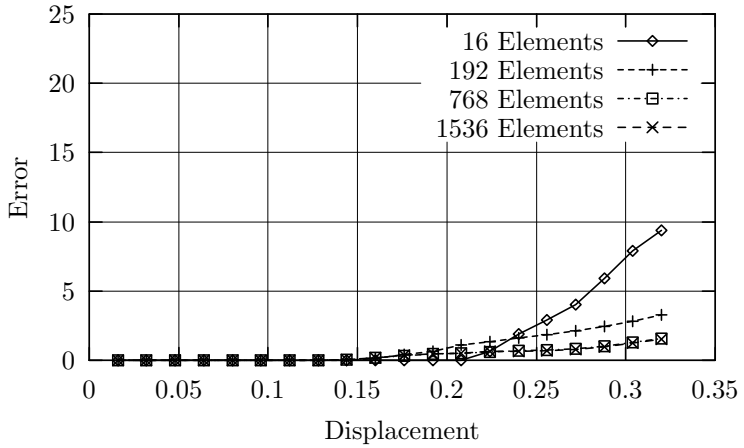

Figure 13. *Square plate with a hole. Evolution of the plastic part of local error near the singular point.*

incompatible modes and in consequence, the estimated error is zero for the the patch test strain modes. It has been applied to linear elasticity, non-linear finite elasticity and von Mises elastic-plastic problems.

The estimator evaluates the error for a standard displacement Galerkin finite element model. For this, it applies an auxiliary enriched solution with assumed strain modes.

The formulation results in an algorithm which is evaluated locally, element by element, without need to global equations nor smoothing techniques. This makes it particularly simple and convenient to use in practice.

The limitations of the proposed approach arise from several factors. Firstly, a key assumption is made with regard to convergence rates (20), for which we do not provide a rigorous proof. Secondly, the error estimate for nonlinear problems is computed as a monotonic increasing

function, which precludes valid error estimates for certain load paths. In particular, no attempt is done to discuss bifurcations or instabilities.

In spite of the above limitations, the representative numerical examples presented show a good performance in practical terms, which is encouraging.

REFERENCES

1. *ABAQUS. Theory Manual*. Hibbitt, Karlsson and Sorensen, Inc, 1998.
2. Armero F, Glaser S. On the formulation of enhanced strain finite elements in finite deformations. *Engineering Computations* 1997; **14**:759–791.
3. BabuškaI, Rheinboldt W. A posteriori error estimates for the finite element method. *International Journal for Numerical Methods in Engineering* 1978; **12**:1597–1613.
4. Barthold F, Schmidt M, Stein E. Error indicators and mesh refinements for finite-element-computations of elastoplastic deformations. *Computational Mechanics* 1998; **22**(3):225–238.
5. Ciarlet P. *The finite element method for elliptic problems*. North Holland, 1978.
6. Gabaldón F. Métodos de elementos finitos mixtos con deformaciones supuestas en elastoplasticidad. Ph.D. thesis, E.T.S. Ingenieros de Caminos, Canales y Puertos. Universidad Politécnica de Madrid. 1999.
7. Gabaldón F and Goicolea, J. Error estimation based on non-linear enhanced assumed strain elements. In *Proocedings of ECCOMAS 2000*. 11–14 September. Barcelona, Spain. 2000.
8. Johnson C, Hansbo P. Adaptive finite element methods in computational mechanics. *Computer Methods in Applied Mechanics and Engineering* 1992; **101**:143–181.
9. Korelc J, Wriggers P. Consistent gradient formulation for a stable enhanced strain method for large deformations.
10. Ortiz M, Quigley J. Adaptive mesh refinement in strain localisation problems. *Computer Methods in Applied Mechanics and Engineering* 1991; **90**:781–804.
11. Ortiz M, Stainier L. The variational formulation of viscoplastic constitutive updates. *Computer Methods in Applied Mechanics and Engineering* 1999; **171**(3–4):419–444
12. Radovitzky R, Ortiz M. Error estimation and adaptive meshing in strongly nonlinear dynamic problems. *Computer Methods in Applied Mechanics and Engineering* 1998; **172**(1–4):203–240.
13. Scordelis A, Lo K. Computer analysis of cylindrical shells. *Journal of American Concrete Institute* 1969; **61**:539–561.
14. Simó J, Armero F. Geometrically nonlinear enhanced strain mixed methods and the method of incompatible modes. *International Journal for Numerical Methods in Engineering* 1992; **33**:1413–1449.
15. Simó J, Armero F, Taylor, R. Improved versions of assumed enhanced strain tri-linear elements for 3d finite deformation problems. *Computer Methods in Applied Mechanics and Engineering* 1993; **110**:359–386.
16. Simó J, Rifai, S. A class of mixed assumed methods and the method of incompatible modes. *International Journal for Numerical Methods in Engineering* 1990; **29**:1595–1638.
17. Stein E, Schmidt M, Barthold F. Theorie und algorithmen adaptiver fe-methoden für elastoplastische deformationen. In *Adaptive finite element methoden in der angewandten mechanik*. 1997.
18. Washizu K. *Variational Methods in Elasticity & Plasticity* (3st edn). Pergamon Press, 1982. *Engineering Computations* 1996; **13**:103–123.
19. Zienkiewicz O, Zhu J. A simple error estimator and adaptive procedure for practical engineering analysis. *International Journal for Numerical Methods in Engineering* 1987; **24**:337–357.